

Forward–backward semiclassical dynamics for condensed phase time correlation functions

Nicholas J. Wright and Nancy Makri^{a)}

Department of Chemistry, University of Illinois, Urbana, Illinois 61801

(Received 6 February 2003; accepted 16 April 2003)

The forward–backward semiclassical dynamics (FBSD) scheme for obtaining time correlation functions shows much promise as a method for including quantum mechanical effects into the calculation of dynamical properties of condensed phase systems. By combining this scheme with a discretized path integral representation of the Boltzmann operator one is able to calculate correlation functions at finite temperature. In this work we develop constant temperature molecular dynamics techniques for sampling the phase space and path integral variables. The resulting methodology is applied to the calculation of the velocity autocorrelation function of liquid argon. At the chosen state point the FBSD results are in good agreement with classical trajectory predictions, but the existence of a non-negligible imaginary part of the correlation function illustrates the importance of proper density quantization even under nearly classical conditions. © 2003 American Institute of Physics. [DOI: 10.1063/1.1580472]

I. INTRODUCTION

One of the long-standing problems in chemical physics is the inclusion of quantum mechanical effects in the dynamics of condensed phase systems. The calculation of the relevant correlation functions is an extremely difficult task. Direct solution of the time-dependent Schrödinger equation is unfeasible because of the well-known exponential scaling with the number of degrees of freedom, and approaches based upon Monte Carlo evaluation of Feynman's path integral method fail because of the "sign problem."

In recent years the use of time-dependent semiclassical theory^{1,2} as a practical way of including quantum mechanical effects into classical molecular dynamics simulations has received renewed attention.^{3–53} The semiclassical approximation provides an attractive method for both practical and fundamental reasons. Because semiclassical mechanics is based on classical trajectories, one can obtain an intuitive understanding of the dynamical process being investigated, as well as taking advantage of the efficient and well-developed molecular dynamics technology.

The use of semiclassical methods has however been plagued by some serious difficulties. Perhaps the most severe of these is again the sign problem, i.e., the inability of Monte Carlo methods to handle oscillatory integrands; such behavior is the hallmark of the semiclassical phase, and the very successful theory of semiclassical algebra^{3,4} is based on stationary phase approximation of integrals involving the semiclassical phase. Forward–backward semiclassical methods^{30–43} provide a practical way to sidestep this problem, albeit with a loss of some quantum mechanical information. These methods combine the two time evolution operators present in the expression for the correlation function into a *single* semiclassical propagator. That step is equivalent to an additional stationary phase approximation in all (or just

some) of the degrees of freedom involved. This approximation reduces the oscillatory character of the integral substantially at the expense of eliminating (at least partially) quantum interference effects. In condensed phase systems the effects of such interference are usually insignificant because of extensive decoherence. In such cases the forward–backward semiclassical approximation is both well-justified and accurate.

Certain forward–backward semiclassical approximations to time correlation functions or expectation values take a quasiclassical form, and recent work^{39,54,55} has incorporated fully quantum mechanical discretized path integral procedures for evaluating the necessary phase space transforms of the Boltzmann operator. This paper is concerned with further developments of the forward–backward semiclassical dynamics (FBSD) method developed in our group,^{35,36} which make the method more efficient as well as compatible with state-of-the-art classical trajectory methods. Specifically, the present paper advances that methodology by developing constant temperature molecular dynamics (MD) algorithms for evaluating the integrals associated with the trajectory initial conditions and path integral variables. The combined MD-FBSD method is applied to the calculation of the velocity autocorrelation functions of a simple one-dimensional anharmonic oscillator and of liquid argon.

Section II reviews the theoretical framework of FBSD for time correlation functions and the imaginary time path integral representation of the Boltzmann operator in a coherent state basis. The path integral expression is converted to one suitable for evaluation via MD, under the assumption that the system is sufficiently ergodic. This procedure, along with various algorithmic details, is described in Sec. III. The applications of the methodology are presented in Sec. IV. Finally, concluding remarks and future directions are given in Sec. V.

^{a)}Electronic mail: nancy@makri.scs.uiuc.edu

II. THEORY: QUASICLASSICAL EXPRESSIONS FROM FORWARD-BACKWARD SEMICLASSICAL DYNAMICS

Throughout this paper we consider correlation functions of the type

$$C_{AB}(t) = Z^{-1} \text{Tr}(e^{-\beta \hat{H}} \hat{A} e^{i\hat{H}t/\hbar} \hat{B} e^{-i\hat{H}t/\hbar}), \tag{2.1}$$

where \hat{H} is the Hamiltonian operator, $\beta = 1/k_B T$ is the reciprocal temperature in units of the Boltzmann constant and $Z = \text{Tr} e^{-\beta \hat{H}}$ is the canonical partition function.

The basic idea is to combine the time evolution operator and its adjoint in Eq. (2.1) into a *single* propagator that describes the evolution of the system to time t and back again to zero time. To do this one must be able to take account of the effect of the \hat{B} operator at the end of the forward evolution part. To date two representations of \hat{B} as a unitary operator have been used: The Fourier method of Miller and co-workers^{31,34} and the derivative formulation, introduced by Shao and Makri.^{35,36} Both the derivative formulation and a particular linearization of the full semiclassical approximation to the correlation function⁵⁶ lead to appealing and practical quasiclassical expressions. In this work we use the derivative formulation,^{35,36,57} where the following identity is used to represent the \hat{B} operator

$$\hat{B} = -i \left. \frac{\partial}{\partial \mu} e^{i\mu \hat{B}} \right|_{\mu=0}. \tag{2.2}$$

The method has been described in detail in previous publications^{35,36,39,40,54} and we only give a brief outline here. The expressions presented below are given for a system of d atoms described by $3d$ Cartesian coordinates, which are denoted collectively by the $3d$ -dimensional vector \mathbf{x} .

After inserting Eq. (2.2) into Eq. (2.1) and using the Herman-Kluk phase space representation¹⁵ of the forward-backward operator $\hat{U} = e^{i\hat{H}t/\hbar} e^{i\mu \hat{B}} e^{-i\hat{H}t/\hbar}$ the Heisenberg transform of \hat{B} in the correlation function takes the form^{35,36,40,57}

$$\begin{aligned} \hat{B}(t) &\equiv -i \left. \frac{\partial}{\partial \mu} e^{i\hat{H}t/\hbar} e^{i\mu \hat{B}} e^{-i\hat{H}t/\hbar} \right|_{\mu=0} \\ &= -i (2\pi\hbar)^{-3d} \frac{\partial}{\partial \mu} \int d\mathbf{x}_0 \int d\mathbf{p}_0 \\ &\quad \times \exp\left(\frac{i}{\hbar} S(\mathbf{x}_0, \mathbf{p}_0)\right) |g(\mathbf{x}_f, \mathbf{p}_f)\rangle \langle g(\mathbf{x}_0, \mathbf{p}_0)| \Big|_{\mu=0}. \end{aligned} \tag{2.3}$$

Here the phase space variables $\mathbf{x}_0, \mathbf{p}_0$ specify initial conditions for classical trajectories, which are first integrated forward to the time t . At that time the trajectories incur position and momentum jumps given by the relations

$$\delta \mathbf{x}_t = -\frac{1}{2} \hbar \mu \frac{\partial}{\partial \mathbf{p}_t} B(\mathbf{x}_t, \mathbf{p}_t), \quad \delta \mathbf{p}_t = \frac{1}{2} \hbar \mu \frac{\partial}{\partial \mathbf{x}_t} B(\mathbf{x}_t, \mathbf{p}_t), \tag{2.4}$$

while the action increments by the amount

$$\delta S_t = \hbar \mu B(\mathbf{x}_t, \mathbf{p}_t) + \mathbf{p}_t \cdot \delta \mathbf{x}_t. \tag{2.5}$$

Subsequently, each trajectory is integrated back to time zero following the classical equations of motion, reaching the phase space point $\mathbf{x}_f, \mathbf{p}_f$, and the total accumulated action has the value S . Finally, $g_{\mathbf{x}_0, \mathbf{p}_0}$ in Eq. (2.3) are coherent states described by complex-valued Gaussians

$$\begin{aligned} \langle \mathbf{x} | g_{\mathbf{x}_0, \mathbf{p}_0} \rangle &= \left(\frac{2}{\pi}\right)^{3d/4} (\det \boldsymbol{\gamma})^{1/4} \exp\left[-(\mathbf{x} - \mathbf{x}_0) \cdot \boldsymbol{\gamma} (\mathbf{x} - \mathbf{x}_0) \right. \\ &\quad \left. + \frac{i}{\hbar} \mathbf{p}_0 \cdot (\mathbf{x} - \mathbf{x}_0)\right], \end{aligned} \tag{2.6}$$

where $\boldsymbol{\gamma}$ is a $3d \times 3d$ matrix.

The notable feature of Eq. (2.3) is the absence of the semiclassical prefactor. Elimination of the latter has been achieved by linearizing the final trajectory values and the action in the infinitesimal parameter μ and rescaling the position and momentum jumps to compensate for the prefactor. For this reason the trajectory increments given in Eq. (2.4) are equal to *one-half* of the values dictated by the classical equations of motion that correspond to the product of exponential operators in Eq. (2.3).^{35,36}

The infinitesimal character of the trajectory jumps at the end of the forward propagation means that the cross terms between distinct forward and backward trajectories have been neglected. Thus, Eq. (2.3) cannot account for quantum interference effects. As stated in the introduction, such effects are strongly quenched in systems of many degrees of freedom. Because of this natural decoherence, FBSD can provide an accurate approximation to condensed phase dynamics.

The above structure also allows transformation of Eq. (2.3) to a derivative-free form that involves trajectories only in the forward time direction.^{42,57} Thus, the Heisenberg operator takes the form

$$\begin{aligned} \hat{B}(t) &= (2\pi\hbar)^{-3d} \int d\mathbf{x}_0 \int d\mathbf{p}_0 B(\mathbf{x}(t), \mathbf{p}(t)) \\ &\quad \times \left((1 + \frac{3}{2}d) |g_{\mathbf{x}_0, \mathbf{p}_0}\rangle \langle g_{\mathbf{x}_0, \mathbf{p}_0}| \right. \\ &\quad \left. - 2(\mathbf{x} - \mathbf{x}_0) \cdot \boldsymbol{\gamma} |g_{\mathbf{x}_0, \mathbf{p}_0}\rangle \langle g_{\mathbf{x}_0, \mathbf{p}_0}(\mathbf{x} - \mathbf{x}_0)| \right), \end{aligned} \tag{2.7}$$

where $B(\mathbf{x}(t), \mathbf{p}(t))$ denotes the classical analogue of the operator. The correlation function then becomes

$$\begin{aligned} C_{AB}(t) &= Z^{-1} (2\pi\hbar)^{-3d} \int d\mathbf{x}_0 \int d\mathbf{p}_0 B(\mathbf{x}(t), \mathbf{p}(t)) \\ &\quad \times \left[(1 + \frac{3}{2}d) \langle g_{\mathbf{x}_0, \mathbf{p}_0} | e^{-\beta \hat{H}} \hat{A} | g_{\mathbf{x}_0, \mathbf{p}_0} \rangle \right. \\ &\quad \left. - 2 \langle g_{\mathbf{x}_0, \mathbf{p}_0} | (\mathbf{x} - \mathbf{x}_0) \cdot e^{-\beta \hat{H}} \hat{A} \boldsymbol{\gamma} (\mathbf{x} - \mathbf{x}_0) | g_{\mathbf{x}_0, \mathbf{p}_0} \rangle \right]. \end{aligned} \tag{2.8}$$

Throughout the rest of the paper it is assumed for simplicity that the matrix $\boldsymbol{\gamma}$ is diagonal and its elements are written as a one-dimensional array γ_{sj} ($s = 1, \dots, d, j = 1, 2, 3$).

The next question to consider is the calculation of the coherent state transform of the Boltzmann operator. This function determines the weights of the initial conditions from

which classical trajectories are launched. It is thus important to use an accurate quantum mechanical representation of this object. The best solution is to represent the Boltzmann operator as an imaginary time path integral.⁵⁸ Just such a procedure was recently developed in our group.^{39,54}

By splitting the Boltzmann operator into a product of N imaginary time slices of length $\Delta\beta = \beta/N$

$$e^{-\beta H} = (e^{-\Delta\beta H})^N, \quad (2.9)$$

using the Trotter factorization of the exponential evolution operator

$$e^{-\Delta\beta \hat{H}} = e^{-\Delta\beta \hat{H}_0/2} e^{-\Delta\beta \hat{V}} e^{-\Delta\beta \hat{H}_0/2}, \quad (2.10)$$

for sufficiently small $\Delta\beta$, and performing some algebra, one arrives at the following discretized path integral representation of the forward-backward semiclassical correlation function⁵⁴ (PI-FBSD):

$$C_{AB}(t) = (2\pi\hbar)^{-3d} \int d\mathbf{x}_0 \int d\mathbf{p}_0 \int d\mathbf{x}_1 \cdots \int d\mathbf{x}_N \\ \times \Theta(\mathbf{x}_0, \mathbf{p}_0, \mathbf{x}_1, \dots, \mathbf{x}_N) \Lambda_{AB}(\mathbf{x}_0, \mathbf{p}_0, \mathbf{x}_1, \dots, \mathbf{x}_N), \quad (2.11)$$

where

$$\Theta(\mathbf{x}_0, \mathbf{p}_0, \mathbf{x}_1, \dots, \mathbf{x}_N) \\ = Z^{-1} \langle g_{\mathbf{x}_0, \mathbf{p}_0} | e^{-\Delta\beta \hat{H}_0/2} | \mathbf{x}_1 \rangle e^{-\Delta\beta V(\mathbf{x}_1)} \\ \times \langle \mathbf{x}_1 | e^{-\Delta\beta \hat{H}_0} | \mathbf{x}_2 \rangle \cdots e^{-\Delta\beta V(\mathbf{x}_N)} \langle \mathbf{x}_N | e^{-\beta \hat{H}_0/2} | g_{\mathbf{x}_0, \mathbf{p}_0} \rangle \\ = Z^{-1} \prod_{s=1}^d \prod_{j=1}^3 \left(\frac{2\gamma_{sj}}{\pi} \right)^{1/2} \frac{m_s}{m_s + \hbar^2 \Delta\beta \gamma_{sj}} \\ \times \left(\frac{m_s}{2\pi\hbar^2 \Delta\beta} \right)^{(N-1)/2} \\ \times \exp \left\{ - \sum_{s=1}^d \sum_{j=1}^3 \left[\frac{m_s}{m_s + \hbar^2 \Delta\beta \gamma_{sj}} \left(\gamma_{sj}(x_{sj,1} - x_{sj,0})^2 \right. \right. \right. \\ \left. \left. \left. + \gamma_{sj}(x_{sj,N} - x_{sj,0})^2 + \frac{i}{\hbar} p_{sj,0}(x_{sj,1} - x_{sj,N}) \right) \right. \right. \\ \left. \left. - \frac{\Delta\beta}{2m_s} p_{sj,0}^2 - \frac{m_s}{2\hbar^2 \Delta\beta} \sum_{k=2}^N (x_{sj,k} - x_{sj,k-1})^2 \right] \right. \\ \left. - \Delta\beta \sum_{k=1}^N V(\mathbf{x}_k) \right\}, \quad (2.12)$$

is the integrand in the path integral representation of the Husimi transform of the Boltzmann operator, and the function Λ depends upon the form of the operator \hat{A} . For example, the autocorrelation function of the $3d$ -dimensional momentum vector \mathbf{p} is given by the expression

$$C_{\mathbf{p}, \mathbf{p}}(t) = Z^{-1} \text{Tr}(e^{-\beta H} \hat{\mathbf{p}} \cdot e^{iHt/\hbar} \hat{\mathbf{p}} e^{-iHt/\hbar}) \\ = (2\pi\hbar)^{-3d} \int d\mathbf{x}_0 \int d\mathbf{p}_0 \int d\mathbf{x}_1 \cdots \int d\mathbf{x}_N \\ \times \Theta(\mathbf{x}_0, \mathbf{p}_0, \mathbf{x}_1, \dots, \mathbf{x}_N) \Lambda_{\mathbf{p}, \mathbf{p}}(\mathbf{x}_0, \mathbf{p}_0, \mathbf{x}_1, \dots, \mathbf{x}_N), \quad (2.13)$$

where

$$\Lambda_{\mathbf{p}, \mathbf{p}}(\mathbf{x}_0, \mathbf{p}_0, \mathbf{x}_1, \dots, \mathbf{x}_N) \\ = (1 + \frac{3}{2}d)\theta(t) - 2 \sum_{s=1}^d \sum_{j=1}^3 \gamma_{sj} f_{sj}^*(x_{sj,0}, p_{sj,0}, x_{sj,1}) \\ \times \left(-i\hbar \frac{m_s}{m_s + \hbar^2 \Delta\beta \gamma_{sj}} p_{sj}(t) \right. \\ \left. + \theta(t) f_{sj}(x_{sj,0}, p_{sj,0}, x_{sj,N}) \right). \quad (2.14)$$

The functions introduced in the last equation are

$$f_{sj}(x_{sj,0}, p_{sj,0}, x_{sj,k}) = \frac{m_s}{m_s + \hbar^2 \Delta\beta \gamma_{sj}} \\ \times \left(x_{sj,k} - x_{sj,0} + i\hbar \frac{\Delta\beta}{2m_s} p_{sj,0} \right) \quad (2.15)$$

and

$$\theta(t) = \sum_{s=1}^d \sum_{j=1}^3 w_{sj}(x_{sj,0}, p_{sj,0}, x_{sj,N}) p_{sj}(t), \quad (2.16)$$

where

$$w_{sj}(x_{sj,0}, p_{sj,0}, x_{sj,k}) = \frac{m_s}{m_s + \hbar^2 \Delta\beta \gamma_{sj}} \\ \times [p_{sj,0} + 2i\hbar \gamma_{sj}(x_{sj,k} - x_{sj,0})]. \quad (2.17)$$

It is instructive to consider for a moment the physical structure of the PI-FBSD expression, which is illustrated schematically in Fig. 1. Each quantum mechanical particle is represented by a ‘‘coherent state bead’’ \mathbf{x}_0 (with an associated momentum \mathbf{p}_0) that is coupled to N ‘‘path integral beads’’ $\mathbf{x}_1 \cdots \mathbf{x}_N$, all connected by harmonic springs. The main difference from the standard classical isomorphism of the imaginary-time path integral⁵⁹ is that the ‘‘necklace’’ of path integral beads is now open, closing through the coherent state bead. The force constants associated with the springs that connect the coherent state bead to the first and last beads of the path integral necklace are different from those between path integral beads. The intermolecular potential acts between the regular path integral beads but has no direct influence upon the coherent state bead. The path integral beads evolve through configuration space, attaining statistical distributions dictated by Eq. (2.11), and their interaction with the coherent state bead determines the appropriate weights of the trajectory initial conditions $\mathbf{x}_0, \mathbf{p}_0$ according to the path integral discretization of the coherent state trans-

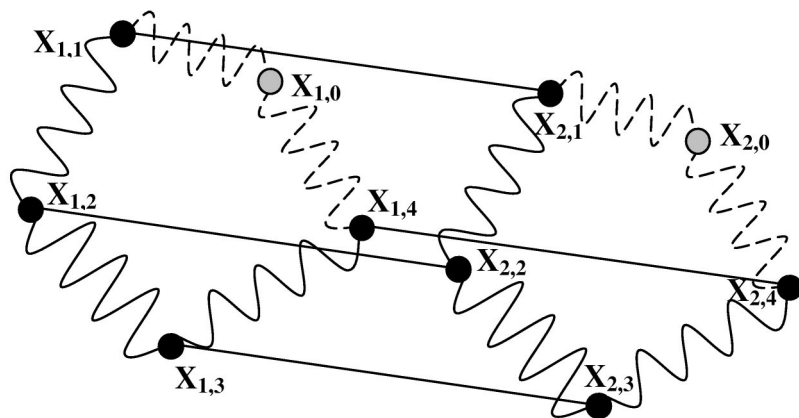


FIG. 1. Schematic representation of combined path integral forward backward representation of the density for two atoms (labeled 1 and 2) for the case $N=4$. The regular path integral beads are depicted by solid circles and the coherent state beads by a gray circle. Intermolecular interactions are indicated by straight lines and spring potentials between beads are represented by wavy lines. Note that the intermolecular potential does not directly affect the coherent state beads and that the spring potentials involving the coherent state bead are different from those involving regular path integral beads.

form of the Boltzmann operator. The time-dependent information $\mathbf{x}_t, \mathbf{p}_t$ is obtained from each initial condition $\mathbf{x}_0, \mathbf{p}_0$ by propagating a constant energy classical trajectory. A related formula for the calculation of rate constants from the reactive flux correlation function was recently described by Yamamoto *et al.*⁵⁵

III. EVALUATION OF PI-FBSD CORRELATION FUNCTIONS USING MOLECULAR DYNAMICS

Multidimensional integrals of the type that appears in the previous section are usually evaluated by Monte Carlo (MC) methods. Such a procedure for PI-FBSD correlation functions has been described in recent work by our group.^{39,54} In this paper we explore an alternative approach based upon the use of molecular dynamics (MD). We do this for several reasons; primarily our desire is to develop a simple, efficient scheme that can be interfaced with modern molecular dynamics techniques straightforwardly. For example, if one wished to study several quantum degrees of freedom interacting with a bath of molecules with rigid bonds, MC methods are much more difficult to apply than MD ones, where standard SHAKE and RATTLE procedures^{60,61} can be used to constrain bond lengths. Further, by combining path integrals with Car-Parrinello *ab initio* molecular dynamics⁶² one can envisage performing on-the-fly forward-backward semiclassical simulations, which would be impossible with Monte Carlo as these *ab initio* methods are inextricably tied to MD.^{63,64}

Many previous studies have been carried out using MD for sampling the multidimensional space of the relevant integration variables. MD sampling methods have also been applied to imaginary-time path integral calculations to evaluate equilibrium properties of many-particle systems. Tuckerman *et al.*⁶⁵ have compared various such algorithms and shown that MD methods are about as efficient as the best Monte Carlo based method.

In order to derive a molecular dynamics algorithm for evaluating Eq. (2.8) we introduce N momenta conjugate to the path integral coordinate variables. Multiplying and dividing by this “kinetic energy”-type Gaussian integral, the correlation function is brought in the form

$$\begin{aligned}
 C_{AB}(t) = & \lambda \int d\mathbf{x}_0 \int d\mathbf{p}_0 \int d\mathbf{x}_1 \int d\mathbf{p}_1 \cdots \int d\mathbf{x}_N \int d\mathbf{p}_N \\
 & \times \exp \left\{ - \sum_{s=1}^d \sum_{j=1}^3 \frac{m_s}{m_s + \hbar^2 \Delta \beta \gamma_{sj}} \left(\gamma_{sj}(x_{sj,1} - x_{sj,0})^2 \right. \right. \\
 & \left. \left. + \gamma_{sj}(x_{sj,N} - x_{sj,0})^2 + \frac{\Delta \beta}{2m_s} p_{sj,0}^2 \right. \right. \\
 & \left. \left. + \frac{i}{\hbar} p_{sj,0}(x_{sj,1} - x_{sj,N}) \right) \right. \\
 & \left. - \beta \sum_{k=1}^N \frac{p_{sj,k}^2}{2\tilde{m}_s} - \frac{m_s}{2\hbar^2 \Delta \beta} \sum_{k=2}^N (x_{sj,k} - x_{sj,k-1})^2 \right. \\
 & \left. - \Delta \beta \sum_{k=1}^N V(\mathbf{x}_k) \right\} \Lambda_{AB}(\mathbf{x}_0, \mathbf{p}_0, \mathbf{x}_1, \dots, \mathbf{x}_N), \quad (3.1)
 \end{aligned}$$

where \tilde{m}_s are arbitrary masses associated with the path integral beads and λ combines all the constants in Eq. (2.12) as well as the factor arising from the Gaussian momentum integral. Ignoring for a moment the imaginary part of the exponent, we have an expression that resembles an equilibrium average for a system of $3d(N+1)$ fictitious classical particles. The Hamiltonian for this classical system is

$$\begin{aligned}
 H_{\text{sample}} = & \sum_{s=1}^d \sum_{j=1}^3 \left[\frac{1}{\beta} \frac{m_s}{m_s + \hbar^2 \Delta \beta \gamma_{sj}} \left(\gamma_{sj}(x_{sj,1} - x_{sj,0})^2 \right. \right. \\
 & \left. \left. + \gamma_{sj}(x_{sj,N} - x_{sj,0})^2 + \frac{\Delta \beta}{2m_s} p_{sj,0}^2 \right) + \sum_{k=1}^N \frac{p_{sj,k}^2}{2\tilde{m}_s} \right. \\
 & \left. + \sum_{k=2}^N \frac{m_s N}{2\hbar^2 \beta^2} (x_{sj,k} - x_{sj,k-1})^2 \right] + \frac{1}{N} \sum_{k=1}^N V(\mathbf{x}_k). \quad (3.2)
 \end{aligned}$$

This Hamiltonian is very similar to that obtained in a molecular dynamics treatment of an imaginary time path integral.⁶⁵ The main difference comes from the presence of the coherent states, which introduce additional terms between the first and the last imaginary time path integral beads. With the above definition the correlation function is rewritten in the following MD-PI-FBSD form

$$C_{AB}(t) = \kappa^{-1} \frac{\int d\mathbf{x}_0 \int d\mathbf{p}_0 \int d\mathbf{x}_1 \int d\mathbf{p}_1 \cdots \int d\mathbf{x}_N \int d\mathbf{p}_N \exp(-\beta H_{\text{sample}}) F_{AB}(\mathbf{x}_0, \mathbf{p}_0, \mathbf{x}_1, \dots, \mathbf{x}_N)}{\int d\mathbf{x}_0 \int d\mathbf{p}_0 \int d\mathbf{x}_1 \int d\mathbf{p}_1 \cdots \int d\mathbf{x}_N \int d\mathbf{p}_N \exp(-\beta H_{\text{sample}})}, \quad (3.3)$$

where

$$F_{AB}(\mathbf{x}_0, \mathbf{p}_0, \mathbf{x}_1, \dots, \mathbf{x}_N) = \exp\left(-\frac{i}{\hbar} \sum_{s=1}^d \sum_{j=1}^3 \frac{m_s}{m_s + \hbar^2 \Delta \beta \gamma_{sj}} p_{sj,0} (x_{sj,1} - x_{sj,N})\right) \Lambda_{AB}(\mathbf{x}_0, \mathbf{p}_0, \mathbf{x}_1, \dots, \mathbf{x}_N) \quad (3.4)$$

and

$$\kappa = \frac{\int d\mathbf{x}_1 \cdots \int d\mathbf{x}_N \sigma(\mathbf{x}_1, \dots, \mathbf{x}_N) \exp(-\sum_{s=1}^d \sum_{j=1}^3 \alpha_{sj} (x_{sj,1} - x_{sj,N})^2)}{\int d\mathbf{x}_1 \cdots \int d\mathbf{x}_N \sigma(\mathbf{x}_1, \dots, \mathbf{x}_N)}. \quad (3.5)$$

The integral in Eq. (3.5) is the normalization constant obtained in earlier work.³⁹ In the last expression

$$\begin{aligned} \sigma(\mathbf{x}_1, \dots, \mathbf{x}_N) &= \exp\left[-\sum_{s=1}^d \sum_{j=1}^3 \left(\frac{m_s \gamma_{sj}/2}{m_s + \hbar^2 \Delta \beta \gamma_{sj}} (x_{sj,1} - x_{sj,N})^2\right.\right. \\ &\quad \left.\left.+ \frac{m_s}{2\hbar^2 \Delta \beta} \sum_{k=2}^N (x_{sj,k} - x_{sj,k-1})^2\right)\right] \\ &\quad \times \exp\left(-\Delta \beta \sum_{k=1}^N V(\mathbf{x}_k)\right) \end{aligned} \quad (3.6)$$

and

$$\alpha_{sj} = \frac{m_s}{2\pi\hbar^2 \Delta \beta} - \frac{m_s \gamma_{sj}/2}{m_s + \hbar^2 \Delta \beta \gamma_{sj}}. \quad (3.7)$$

Equation (3.3) is in the form of a thermodynamic average with respect to a normalized sampling function defined by H_{sample} .

By allowing the system to evolve at temperature $1/k_B\beta$ under the Hamiltonian H_{sample} we generate initial conditions $\mathbf{x}_0, \mathbf{p}_0$ for the classical trajectories and values of the positions of the path integral beads, $\mathbf{x}_1, \dots, \mathbf{x}_N$. Then for each initial condition $\mathbf{x}_0, \mathbf{p}_0$ a constant energy classical trajectory is propagated to obtain the time-dependent information $\mathbf{x}_t, \mathbf{p}_t$.

To calculate the time evolution of the Hamiltonian H_{sample} we must use a technique that generates trajectories whose time average is equal to the canonical ensemble average. We adopt the Nosé–Hoover chains method⁶⁶ used by Tuckerman *et al.*⁶⁵ in their study of path integral molecular dynamics methods. The original Nosé–Hoover^{67,68} method is not adequate for this system where the effective potential in the path integral variables consists of harmonic terms, as it is known that the former does not produce the correct averages in the case of a one-dimensional harmonic oscillator.⁶⁶

A Nosé–Hoover chain of length two was attached to every degree of freedom in the system. To integrate the resulting equations of motion we used the velocity Verlet based algorithm of Jang and Voth.⁶⁹ Again in a very similar manner to the previous work of Tuckerman *et al.*⁶⁵ we employed the reversible reference system propagator algorithm⁷⁰ (RESPA) to eliminate problems associated with the different time scales of motion of the harmonic interactions and the intermolecular interactions. In this preliminary application we do

not use any schemes such as staging^{65,71} or normal mode transformations to narrow the frequency range present in the problem, although in future applications their use may be advantageous.

In contrast to Monte Carlo algorithms, where only the values of the coherent state parameters are needed, several more parameters need to be optimized for the solution of the equations using molecular dynamics. These are the two RESPA time steps Δt and $\delta t = \Delta t/n$ (where n is an integer), the masses \tilde{m}_s associated with the path integral beads, and the masses M_s of the Nosé–Hoover thermostats. The values of \tilde{m}_s and M_s must be chosen so that the motion of the path integral beads and the thermostats occur on the same time scale as the motion of the remaining variables of the system. In the calculations presented below we set these masses equal to those of the atoms involved in the calculation. The time steps are chosen to be as large as possible whilst still conserving energy.

To evaluate the normalization constant for the integral we simply set $A=B=1$ and $t=0$ and evaluate Eq. (3.3) as described above. The relevant function in the integrand has the form

$$\begin{aligned} \Lambda_{11}(\mathbf{x}_0, \mathbf{p}_0, \mathbf{x}_1, \dots, \mathbf{x}_N) &= (1 + \frac{3}{2}d) - 2 \sum_{s=1}^d \sum_{j=1}^3 \gamma_{sj} f_{sj}^*(x_{sj,0}, p_{sj,0}, x_{sj,1}) \\ &\quad \times f_{sj}(x_{sj,0}, p_{sj,0}, x_{sj,N}). \end{aligned} \quad (3.8)$$

The evaluation of the normalization constant was previously carried out by performing a separate calculation of an additional, different integral by Monte Carlo.^{39,54} In this work we use a simpler approach, which has the advantage of requiring the same sampling function as the time-dependent calculation, so only minimal additional computation is involved. Note that for the case $N=1$ the normalization factor $\kappa=1$ so under these circumstances it does not need to be evaluated.

Note that the MD algorithm developed here (and the original MC algorithm) is easily parallelized; one simply propagates a trajectory under H_{sample} with different initial conditions on each processor. Communication between processors is only required at the end of the run to collect the results, which means almost perfect scaling efficiency is achieved as the number of processors is increased.

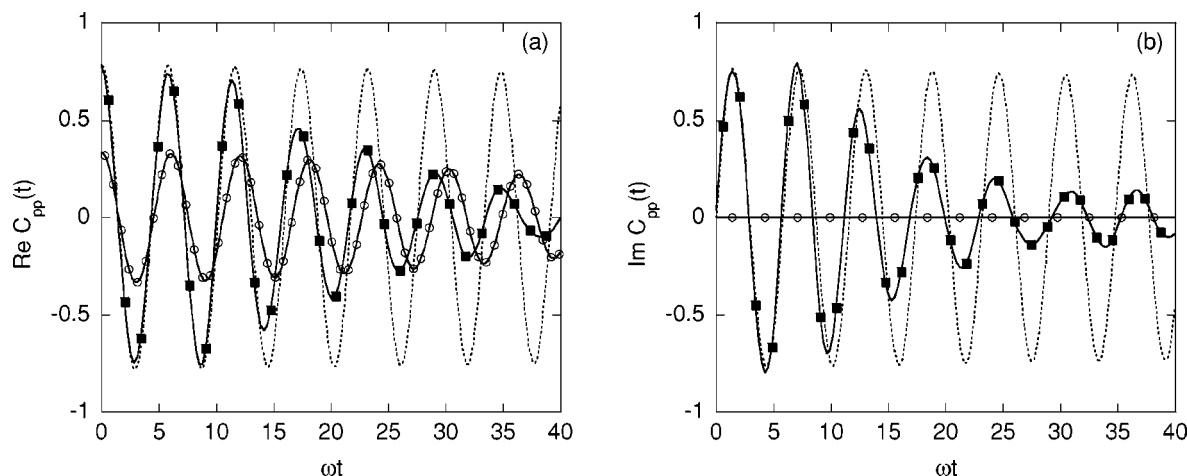


FIG. 2. The real (a) and imaginary (b) parts of the momentum autocorrelation function for the one-dimensional anharmonic oscillator given in Eq. (4.1) for $\hbar\omega\beta=3\sqrt{2}$. Dashed line: Exact quantum mechanical result obtained via a basis set calculation. Solid squares: MD-PI-FBSD results. Hollow circles: Results of fully classical simulation.

IV. NUMERICAL APPLICATIONS

In this section we present numerical tests of the molecular dynamics methodology described in Secs. II and III. The first test involves a simple one-dimensional anharmonic oscillator described by the potential

$$V(x) = \frac{1}{2}m\omega^2x^2 - 0.1x^3 + 0.1x^4, \quad (4.1)$$

with $m=1$ and $\omega=\sqrt{2}$. As discussed previously^{35,39,42} this potential is very anharmonic, causing the wave packet to dephase within a few vibrational periods. The forward-backward method describes this dephasing semiquantitatively; however, it was found to be incapable of accounting for the rephasing that occurs at later times due to coherence effects.

Figure 2 shows the comparison between the exact quantum result, the MD-PI-FBSD results and the classical result for the momentum correlation function at a low temperature, $\hbar\omega\beta=3\sqrt{2}$. The FBSD results converged with 12 path integral beads and $\sim 30\,000$ trajectories were necessary to reduce the statistical error to about 1%. The results obtained using

the MD-PI-FBSD method agree well with those obtained from a Monte Carlo calculation (not shown), indicating that the new MD method correctly samples the integration space. As was discussed previously, the forward-backward correlation function decays too rapidly but maintains the same frequency as the quantum result for several periods, in contrast to the classical one. This means after Fourier transforming the short time signal the FBSD result will have a peak at the correct frequency whereas the classical one will not. It also implies that in systems where quantum mechanical effects are important, but the dynamics are dissipative and therefore intrinsically short time, FBSD will reproduce the correct quantum correlation function.

Figure 3 shows the same comparison at a high temperature, $\hbar\omega\beta=\sqrt{2}/10$. Here only one path integral bead was required. At this temperature the FBSD results are essentially exact. As one confirms by examining the analytical expression for a harmonic oscillator, the real part of a correlation function approaches the classical result faster than the imaginary part. This behavior is seen clearly in Fig. 3(b), where

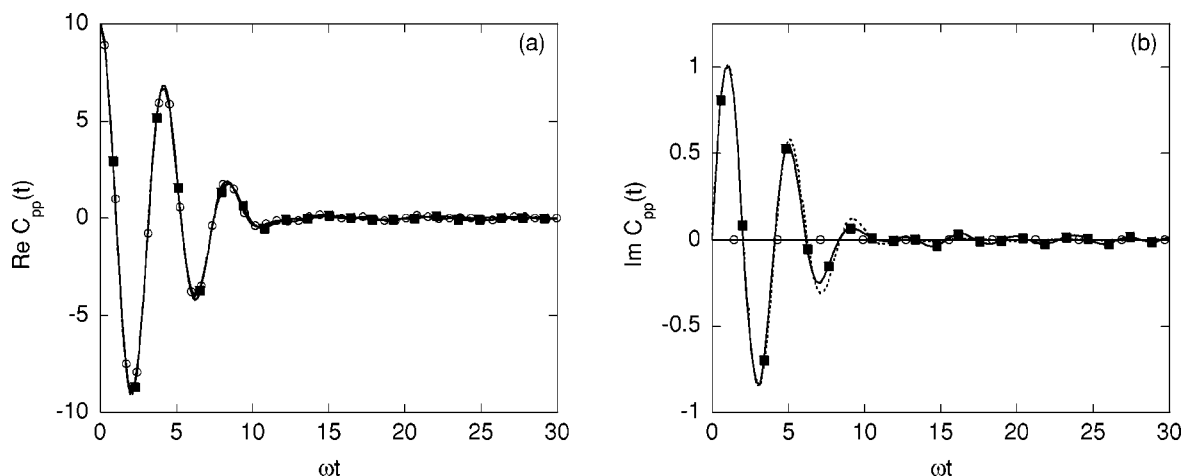


FIG. 3. The real (a) and imaginary (b) parts of the momentum autocorrelation function for the one-dimensional anharmonic oscillator given in Eq. (4.1) for $\hbar\omega\beta=0.1\sqrt{2}$. Dashed line: Exact quantum mechanical result obtained via a basis set calculation. Solid squares: MD-PI-FBSD results. Hollow circles: Results of fully classical simulation.

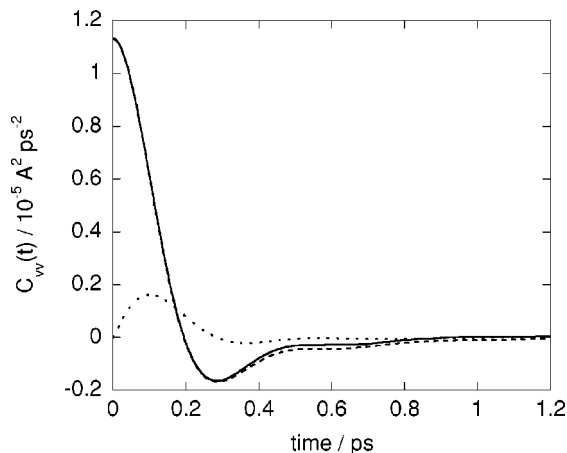


FIG. 4. Velocity autocorrelation function for liquid argon under conditions described in Sec. IV. The solid, dotted and dashed lines show the FBSD (real and imaginary components) and classical results, respectively.

classical mechanics predicts the real part of the correlation function essentially quantitatively, but the imaginary part amounts to about 10% of the maximum value of the real part.

Next we present a benchmark application of the MD-PI-FBSD method to liquid argon. The calculation is performed at 183 K, at a density of 1.60 g cm^{-3} upon a cubic unit cell containing 108 atoms under periodic boundary conditions. All interactions are truncated at half of the unit cell dimension and are described by a Lennard-Jones potential of the type

$$V(r) = 4\varepsilon \left[\left(\frac{\sigma}{r} \right)^{12} - \left(\frac{\sigma}{r} \right)^6 \right], \quad (4.2)$$

with $\varepsilon = 85 \text{ cm}^{-1}$ and $\sigma = 3.4 \text{ \AA}$, where r represents the interatomic separation. At this state point the dynamics are presumed classical and thus a single imaginary time path integral bead was used.

The choice of γ , the coherent state parameter, is not entirely straightforward for a condensed phase simulation. In this work we ran two independent calculations, one using the value γ_ω suggested by the harmonic frequency obtained from the pair potential, and another using $\gamma_\omega/2$. As the two calculations agreed with each other and with the classical result (*vide infra*) we did not explore this issue further, but we note that further investigation may be required in the case of more complex molecular fluids. Approximately one million trajectories were required to obtain converged results for the velocity autocorrelation function, which is obtained from Eq. (2.13) by dividing by the appropriate mass factor for Ar, i.e.,

$$C_{\mathbf{v},\mathbf{v}}(t) = C_{\mathbf{p},\mathbf{p}}(t)/m_{\text{Ar}}^2. \quad (4.3)$$

Figure 4 shows the comparison between the correlation function obtained classically and that obtained from the MD-PI-FBSD calculation. The real parts exhibit good agreement with one another, indicating that the MD-PI-FBSD calculation is behaving correctly. The integrated value of the MD-PI-FBSD time correlation function that yields the self-diffusion constant is in reasonable agreement with the

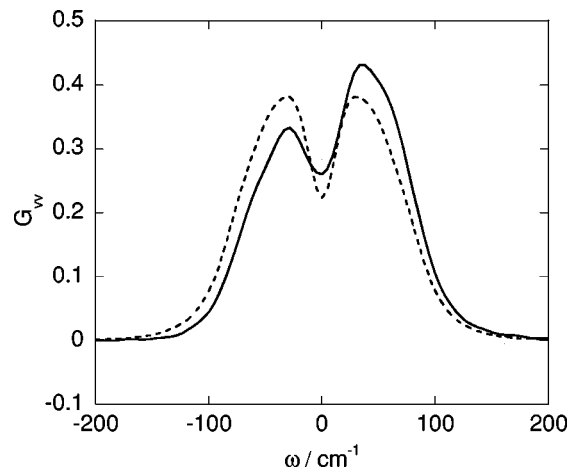


FIG. 5. Fourier transform of the velocity autocorrelation function for liquid argon displayed in Fig. 4. The solid and dashed lines show the FBSD and classical results, respectively.

corresponding classical result. However, the FBSD calculation also produces the imaginary component of the correlation function, which reaches a height equal to about 15% of the maximum value of the real part.

Figure 5 shows the Fourier transforms

$$G_{\mathbf{v},\mathbf{v}}(\omega) = \frac{1}{2\pi} \int_{-\infty}^{\infty} C_{\mathbf{v},\mathbf{v}}(t) e^{i\omega t} dt, \quad (4.4)$$

of the FBSD and classical correlation functions. By virtue of its nonzero imaginary part, the FBSD transform (in contrast to the classical result) is *not* symmetrical about $\omega = 0$. This asymmetry is a well-known manifestation of the detailed balance relation, i.e.,

$$G_{\mathbf{v},\mathbf{v}}(-\omega) = e^{-\beta\hbar\omega} G_{\mathbf{v},\mathbf{v}}(\omega), \quad (4.5)$$

which the calculated MD-PI-FBSD result satisfies to a very good approximation. Purely classical MD simulations cannot directly capture imaginary components and the resulting asymmetry in Fourier space. Note we have obtained the imaginary part of the correlation function without making any assumptions, such as those involved in applying “quantum correction factors” to classical correlation functions.^{72–74}

V. CONCLUSIONS

We have developed a MD-based method for evaluating correlation functions arising from the previously developed PI-FBSD method. The present scheme is based upon using constant temperature molecular dynamics (as opposed to the traditional Monte Carlo based methods) to sample the initial conditions of the classical trajectories. The method is straightforward to implement and provides an efficient tool for the calculation of correlation functions in large clusters, liquids, or biological systems. The method is also very easy to implement on modern parallel computer architecture, as hardly any communication between processors is required.

As a preliminary test we have applied the method to the calculation of the velocity correlation function of liquid ar-

gon. Despite the large number of degrees of freedom present in the problem the calculation of the correlation function was quite straightforward and no excessive computational effort was required. The calculated correlation function shows good agreement with that obtained from classical mechanics but, in contrast to the classical one, possesses a non-negligible imaginary part. This feature is essential for the accurate prediction of spectroscopic intensities or relaxation rates and should enable us in the future to improve force fields for molecular liquids by comparison of simulation results with experiment.

The $N=1$ (single path integral bead) limit of the path integral expression for the Boltzmann operator is usually regarded as its classical limit. In fact, it is easy to show that the path integral representation of the partition function reverts precisely to the classical result if a single bead is used. By contrast, the present PI-FBSD formulation retains important nonclassical features such as imaginary components even in its crudest ($N=1$) limit. These quantum effects are captured in spite of the absence of phase factors from the integrand. Under less classical conditions one would have to increase the number of path integral beads to achieve convergence. This can be a demanding task, because the complex phase in the FBSD expression disappears only in the single bead limit. While this phase is slowly varying and amounts to very small negative components in one dimension, the problem becomes worse at an exponential rate as the dimensionality of the problem increases. As demonstrated through recent calculations,⁵⁴ the method remains robust and efficient in systems with a few tens of degrees of freedom even with several path integral beads per coordinate. Thus, PI-FBSD simulations of medium-size clusters or light particles in molecular liquids where only 10–20 atoms exhibit highly quantum mechanical behavior (while the remaining particles are treated with a single path integral bead) are currently feasible with modest amounts of computational effort. However, simulations with hundreds of quantum mechanical particles appear challenging at the moment. Our group is currently pursuing efficient ways of dealing with this problem in order to enable the application of the PI-FBSD methodology to low-temperature fluids.

ACKNOWLEDGMENTS

This work was supported by the National Science Foundation under award No. CHE-0212640. Some of the calculations presented were facilitated by the National Computational Science Alliance under Grant No. CHE020053N. N.M. thanks Professor James L. Skinner for stimulating discussions and a critical reading of the manuscript.

¹J. H. Van Vleck, Proc. Natl. Acad. Sci. U.S.A. **14**, 178 (1928).

²C. Morette, Phys. Rev. **81**, 848 (1952).

³W. H. Miller, Adv. Chem. Phys. **25**, 69 (1974).

⁴W. H. Miller, Adv. Chem. Phys. **30**, 77 (1975).

⁵E. J. Heller, J. R. Reimers, and G. Drolshagen, Phys. Rev. A **36**, 2613 (1987).

⁶M. S. Child, *Semiclassical mechanics with molecular applications* (Clarendon, Oxford, 1991).

⁷E. J. Heller, J. Chem. Phys. **94**, 2723 (1991).

⁸S. Tomsovic and E. J. Heller, Phys. Rev. Lett. **67**, 664 (1991).

- ⁹M. A. Sepulveda, S. Tomsovic, and E. J. Heller, Phys. Rev. Lett. **69**, 402 (1992).
- ¹⁰M. A. Sepulveda and F. Grossmann, Adv. Chem. Phys. **XCVI**, 191 (1996).
- ¹¹J. Cao and G. A. Voth, J. Chem. Phys. **104**, 273 (1996).
- ¹²F. Grossmann, Phys. Rev. A **60**, 1791 (1999).
- ¹³S. Garashchuk, F. Grossmann, and D. Tanner, J. Chem. Soc., Faraday Trans. **93**, 781 (1997).
- ¹⁴S. Garashchuk and J. C. Light, J. Chem. Phys. **113**, 9390 (2000).
- ¹⁵M. F. Herman and E. Kluk, Chem. Phys. **91**, 27 (1984).
- ¹⁶E. Kluk, M. F. Herman, and H. L. Davis, J. Chem. Phys. **84**, 326 (1986).
- ¹⁷G. Campolieti and P. Brumer, Phys. Rev. A **50**, 997 (1994).
- ¹⁸J. Wilkie and P. Brumer, Phys. Rev. A **61**, 064101 (2001).
- ¹⁹K. G. Kay, J. Chem. Phys. **100**, 4377 (1994).
- ²⁰K. G. Kay, J. Chem. Phys. **100**, 4432 (1994).
- ²¹K. Kay, J. Chem. Phys. **107**, 2313 (1997).
- ²²A. R. Walton and D. E. Manolopoulos, Mol. Phys. **84**, 961 (1996).
- ²³M. L. Brewer, J. S. Hulme, and D. E. Manolopoulos, J. Chem. Phys. **106**, 4832 (1997).
- ²⁴R. Hernandez and G. A. Voth, Chem. Phys. **233**, 243 (1998).
- ²⁵B. R. McQuarrie and P. Brumer, Chem. Phys. Lett. **319**, 27 (2000).
- ²⁶H. Wang, D. E. Manolopoulos, and W. H. Miller, J. Chem. Phys. **115**, 6317 (2001).
- ²⁷X. Sun and W. H. Miller, J. Chem. Phys. **106**, 916 (1997).
- ²⁸H. Wang, X. Sun, and W. H. Miller, J. Chem. Phys. **108**, 9726 (1998).
- ²⁹X. Sun, H. Wang, and W. H. Miller, J. Chem. Phys. **109**, 4190 (1998).
- ³⁰N. Makri and K. Thompson, Chem. Phys. Lett. **291**, 101 (1998).
- ³¹W. H. Miller, Faraday Discuss. **110**, 1 (1998).
- ³²K. Thompson and N. Makri, J. Chem. Phys. **110**, 1343 (1999).
- ³³K. Thompson and N. Makri, Phys. Rev. E **59**, R4729 (1999).
- ³⁴X. Sun and W. H. Miller, J. Chem. Phys. **110**, 6635 (1999).
- ³⁵J. Shao and N. Makri, J. Phys. Chem. **103**, 7753 (1999).
- ³⁶J. Shao and N. Makri, J. Phys. Chem. **103**, 9479 (1999).
- ³⁷H. Wang, M. Thoss, and W. H. Miller, J. Chem. Phys. **112**, 47 (2000).
- ³⁸J. Shao and N. Makri, J. Chem. Phys. **113**, 3681 (2000).
- ³⁹E. Jezek and N. Makri, J. Phys. Chem. **105**, 2851 (2001).
- ⁴⁰N. Makri, in *Fluctuating paths and fields*, edited by W. Janke, A. Pelster, H.-J. Schmidt, and M. Bachmann (World Scientific, Singapore, 2001).
- ⁴¹H. Wang, M. Thoss, K. L. Sorge, R. Gelabert, X. Gimenez, and W. H. Miller, J. Chem. Phys. **114**, 2562 (2001).
- ⁴²M. Thoss, H. Wang, and W. H. Miller, J. Chem. Phys. **114**, 9220 (2001).
- ⁴³Y. Zhao and N. Makri, Chem. Phys. **280**, 135 (2002).
- ⁴⁴X. Sun and W. H. Miller, J. Chem. Phys. **108**, 8870 (1998).
- ⁴⁵V. Batista, M. T. Zanni, J. Greenblatt, D. M. Neumark, and W. H. Miller, J. Chem. Phys. **110**, 3736 (1999).
- ⁴⁶M. T. Zanni, V. S. Batista, J. Greenblatt, W. H. Miller, and D. M. Neumark, J. Chem. Phys. **110**, 3748 (1999).
- ⁴⁷D. E. Skinner and W. H. Miller, J. Chem. Phys. **111**, 10787 (1999).
- ⁴⁸M. Thoss, W. H. Miller, and G. Stock, J. Chem. Phys. **112**, 10282 (2000).
- ⁴⁹E. A. Coronado, V. S. Batista, and W. H. Miller, J. Chem. Phys. **112**, 5566 (2000).
- ⁵⁰V. Guallar, V. S. Batista, and W. H. Miller, J. Chem. Phys. **113**, 9510 (2000).
- ⁵¹W. H. Miller, J. Phys. Chem. **105**, 2942 (2001).
- ⁵²R. Gelabert, X. Giménez, M. Thoss, H. Wang, and W. H. Miller, J. Chem. Phys. **114**, 2572 (2001).
- ⁵³M. Ovchinnikov, V. A. Apkarian, and G. A. Voth, J. Chem. Phys. **114**, 7130 (2001).
- ⁵⁴N. Makri, J. Phys. Chem. B **106**, 8390 (2002).
- ⁵⁵T. Yamamoto, H. B. Wang, and W. H. Miller, J. Chem. Phys. **116**, 7335 (2002).
- ⁵⁶X. Sun, H. Wang, and W. H. Miller, J. Chem. Phys. **109**, 7064 (1998).
- ⁵⁷N. Makri and J. Shao, in *Accurate description of low-lying electronic states and potential energy surfaces*, edited by M. Hoffmann (Oxford University Press, 2002).
- ⁵⁸R. P. Feynman, *Statistical Mechanics* (Addison-Wesley, Redwood City, 1972).
- ⁵⁹D. Chandler and P. G. Wolynes, J. Chem. Phys. **74**, 4078 (1981).
- ⁶⁰H. C. Anderson, J. Comput. Phys. **52**, 24 (1983).
- ⁶¹J. P. Ryckaert, G. Ciccotti, and H. J. C. Berendsen, J. Comput. Phys. **23**, 327 (1977).
- ⁶²R. Car and M. Parrinello, Phys. Rev. Lett. **55**, 2471 (1985).
- ⁶³M. Tuckerman, D. Marx, M. L. Klein, and M. Parrinello, J. Chem. Phys. **104**, 5579 (1996).

- ⁶⁴D. Marx and M. Parrinello, *J. Chem. Phys.* **104**, 4077 (1996).
- ⁶⁵M. Tuckerman, B. J. Berne, G. J. Martyna, and M. L. Klein, *J. Chem. Phys.* **99**, 2796 (1993).
- ⁶⁶G. J. Martyna, M. L. Klein, and M. Tuckerman, *J. Chem. Phys.* **97**, 2635 (1992).
- ⁶⁷S. Nose, *J. Chem. Phys.* **81**, 511 (1984).
- ⁶⁸W. G. Hoover, *Phys. Rev. A* **31**, 1695 (1985).
- ⁶⁹S. Jang and G. A. Voth, *J. Chem. Phys.* **107**, 9514 (1997).
- ⁷⁰M. Tuckerman, B. J. Berne, and G. J. Martyna, *J. Chem. Phys.* **97**, 1990 (1992).
- ⁷¹M. Sprik, M. L. Klein, and D. Chandler, *Phys. Rev. B* **31**, 4234 (1985).
- ⁷²S. A. Egorov and J. L. Skinner, *Chem. Phys. Lett.* **293**, 469 (1998).
- ⁷³S. A. Egorov, K. F. Everitt, and J. L. Skinner, *J. Phys. Chem.* **103**, 9494 (1999).
- ⁷⁴L. Frommhold, *Collision-induced adsorption in gases* (Cambridge University Press, Cambridge, 1993).